Desalination and Water Treatment
www.deswater.com

doi: 10.5004/dwt.2019.23675

144 (2019) 233–242
March

Fabrication and characterization of magnetic cobalt ferrite nanoparticles for efficient removal of humic acid from aqueous solutions

Mohammad Kamranifar[a], Fatemehsadat Masoudi[b], Ali Naghizadeh[a,*], Majid Asri[c]

[a]*Medical Toxicology and Drug Abuse Research Center (MTDRC), Birjand University of Medical Sciences (BUMS), Birjand, Iran, Tel. +985632381665; Fax: +985632395346; emails: al.naghizadeh@yahoo.com (A. Naghizadeh), mo.kamrani@yahoo.com (M. Kamranifar)*
[b]*Department of Environment Health Engineering, Student Research Committee, Birjand University of Medical Sciences, Birjand, Iran, email: Ftmmasoudi71@yahoo.com*
[c]*Department of Environmental Health Engineering, Faculty of Medicine Sciences, Islamic Azad University, Birjand Branch, Birjand, Iran, email: majid.asri@yahoo.com*

Received 13 June 2018; Accepted 23 December 2018

ABSTRACT

In the present study, magnetic cobalt ferrite nanoparticles were synthesized and its efficiency in removing humic acid from aqueous solutions was investigated. Structural characteristics of magnetic cobalt ferrite nanoparticles by scanning electron microscopy, transmission electron microscopy, Fourier transform infrared spectroscopy, X-ray diffraction and vibrating-sample magnetometerwere described. In addition, the effects of various parameters such as pH (3–11), adsorption dose (0.2–0.8 g/L), contact time (5–90 min), humic acid concentration (5–40 mg/L) and temperature (283–313 K) on the adsorption of humic acid by magnetic cobalt ferrite nanoparticles were studied. The adsorption parameters were determined with Langmuir, Freundlich, Temkin, BET and Dubinin–Radushkevich isotherms as well as pseudo-first and pseudo-second-order kinetics. Finally, the thermodynamic parameters (ΔH, ΔS and ΔG) were investigated. The results of this study showed that in optimum conditions, the maximum adsorption capacity of magnetic cobalt ferrite nanoparticles was 146 mg/g (optimal conditions: pH = 3, adsorbent dose = 0.2 g/L, initial concentration of humic acid = 40 mg/L, contact time = 20 min, temperature = 283 K). The adsorption isotherm data well match with Langmuir and Freundlich models. The kinetics of the process was described well with the pseudo-second-order model. The results of the thermodynamic analysis showed that the values of ΔS and ΔH are positive and ΔG is negative.

Keywords: Magnetic nanoparticles; Cobalt ferrite; Humic acid; Isotherm; Kinetics; Thermodynamics

1. Introduction

Natural organic matter (NOM) is one of the materials in surface water, land and water [1]. This material in the environment is divided into two main categories of compounds, such as proteins, polysaccharides, nucleic acids, etc., and humic substances [2]. Humic acid (HA) is an important ingredient in organic matter that is released from the degradation of plant and animal to the aquatic environments [3,4]. The concentration of humic substances varies regarding to region. Usually in natural water, the concentration of HA is between 0.1 and 10 mg/L [3]. The chemical structure of HA is shown in Fig. 1.

The presence of HA in aquatic environments may cause serious environmental and health problems. For example, HA may cause undesirable color and taste in water, corrosion of metals, reduction in membrane efficiency and

* Corresponding author.

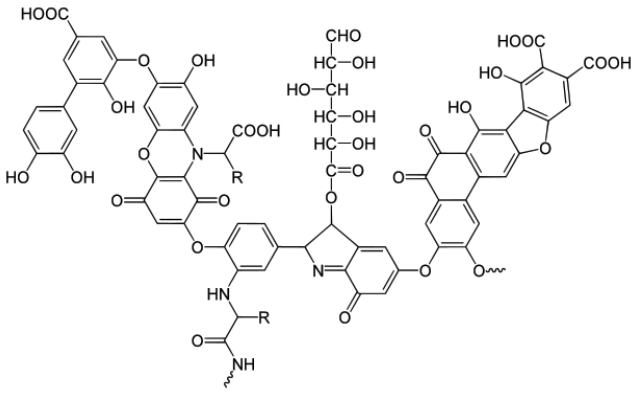

Fig. 1. Humic acid structure [5].

rejuvenation of microorganisms. In addition, HA may react with chlorine disinfectants and produce carcinogenic by-products (trihalomethanes and haloacetic acids) [6,7]. In addition, epidemiologists have recently focused on the reproductive sequelae of trihalomethanes, such as spontaneous abortion, stillbirths, and intra-uterine growth retardation [8]. The most important potential factor for the formation of trihalomethanes is the presence of precursors in water, among which the most important are HAs. Humics are highly complex and heterogeneous compounds of high molecular weight organic matter with various active groups (carboxyl and phenol) and aromatic nuclei, which are caused by the chemical and biological degradation of tissues of plants and animals (such as lignin) [9].

Therefore, the minimization of trihalomethane precursors or the effective elimination of organic matter, including HA, is a crucial issue in the production of high-quality drinking water [10]. Until now, different processes have been used for the removal of organic matter. Conventional processes such as coagulation, sedimentation, filtration, ion exchange, photocatalytic degradation and adsorption have been used to reduce the organic matter of water [11,12]. Often, these methods are faced with problems such as low efficiency, high costs, and the production of by-products [13]. Among the above-mentioned methods, surface adsorption is one of the best and most widely used methods for water and wastewater treatment due to its ease of use and high efficiency. Surface adsorption is a process which has advantages such as low initial cost, flexibility and design simplicity, ease of operation, non-susceptibility to toxic contaminants and reduction of secondary harmful substances production in comparison with other methods [14]. Accordingly, many adsorbents for the removal of HA have been investigated, including chitosan [15], magnetic multi-walled carbon nanotubes [16], magnetic polyaniline [17], polypyrrole-coated granules [18] and activated carbon [19].

One of the important problems in the use of adsorbents is their separation and recovery. In recent years, to solve the problem of separation and recovery of powdered adsorbents, magnetic separation technology has attracted a lot of attention as an alternative method [17]. These magnetite nanoparticles can adsorb contaminants from aqueous solutions and then separate them with a simple magnetic process [20]. One of the types of magnetic nanoparticles is bimetallic nanoparticles and due to its synergistic effects between two metals have certain chemical and physical properties, which make them highly desirable for industrial applications, especially as catalyst. Magnetic nanoparticles of cobalt ferrite ($CoFe_2O_4$) are one of the most important oxide-based spinel ferrite species. These ferromagnetic nanoparticles can be classified as highly recyclable and reusable catalysts, which can easily be separated by an external magnetic field [21]. Also, cobalt ferrite is a cubic spinel ferrite that has advantages such as good magnetism, good chemical and thermal stability, and high mechanical stability [22,23].

The present study was carried out for the synthesis of magnetic cobalt ferrite nanoparticles and surveys the removal of HA from aqueous solutions. In the adsorption process, various parameters such as pH, adsorbent dose, contact time, HA concentration, temperature and thermodynamics of the process were studied. Finally, the isotherm and kinetics of adsorption were studied.

2. Materials and methods

2.1. Synthesis of magnetic cobalt ferrite nanoparticles ($CoFe_2O_4$)

0.001 mol of cobalt nitrate ($Co(NO_3)_2{\cdot}6H_2O$) and 0.012 mol of iron nitrate ($Fe(NO_3)_3{\cdot}9H_2O$) dissolved in 100 mL of deionized water, and then 20 mL of 1 mol of NaOH is added slowly. The solution is then placed at 80°C for 2 h. Subsequently, the formed nanoparticles were separated with the external magnet and placed in the oven after washing with distilled water [24]. Then, the characteristics of nanoparticles produced by scanning electron microscopy (SEM), transmission electron microscopy (TEM), Fourier transform infrared spectroscopy (FTIR), X-ray diffraction (XRD) and vibrating-sample magnetometer (VSM) were investigated.

2.2. Adsorption experiments

This is an experimental study which was carried out on a laboratory scale. HA with a purity of 54% was obtained from Acros Corporation, USA. Also, other materials including $Fe(NO_3)_3.9H_2O$, $Co(NO_3)_2.6H_2O$, HCl, NaOH were purchased from Merck Company , Germany. In adsorption experiments, 500 mg/L of stock solution of HA was prepared by dissolving the HA powder in distilled water. Then, the various parameters such as pH (3–11), adsorbent dose (0.2–0.8 g/L), concentration of HA (5–40 mg/L), contact time (5–90 min) and temperature (283–313 K) were investigated.

It should be noted that pH adjustment was performed using pH meter (HQ411d, Hach, USA) and HCl and NaOH (1 and 0.1 N). Shaker (Multi shaker, Model NB-101MT, Korea) was used for mixing and proper contact of HA and adsorbent at 250 rpm. Separation of the adsorbent from the solution was performed using a magnet. Then, to ensure complete removal of the nanoparticles from the solution, the upper portion of the solution was centrifuged and passed through a membrane filter of 0.45 microns. Finally, the residual HA concentration was measured using a spectrophotometer (UV/VIS spectrophotometer T80$^+$, PG Instrument Ltd.) at 254 nm wavelength.

The amount of HA adsorbed on the adsorbent (adsorption capacity) was performed using Eq. (1).

$$q_e = \frac{C_0 - C_e}{m} \times V \quad (1)$$

where q_e is the adsorption capacity (mg/g), C_0 is the initial concentration (mg/L), C_e is the residual concentration (mg/L), m is the adsorbent dose (g) and V is the sample volume (L) [25].

2.3. Effect of temperature and thermodynamics process

In order to evaluate the effect of temperature on the process of adsorption of HA on cobalt ferrite nanoparticles, the removal efficiency of HA under optimum conditions (pH, adsorbent dose, HA concentration and contact time) at a temperature range of 313–283 K was investigated. For this purpose, an incubator shaker device (Incubator shaker, Model SI-100R, Korea) was used. Eqs. (2)–(4) were used to study the thermodynamics of HA adsorption by magnetic cobalt ferrite nanoparticles.

$$k_d = \frac{q_e}{C_e} \quad (2)$$

$$\Delta G^\circ = -RT \ln k_d \quad (3)$$

$$\ln k_d = -\frac{\Delta H^\circ}{RT} + \frac{\Delta S^\circ}{R} \quad (4)$$

where k_d is the thermodynamic equilibrium constant, T (K) is absolute temperature and R (8.314 J/molK) is the universal constant of the gases [26].

2.4. Study of adsorption isotherm

In this stage, Langmuir, Freundlich, Tamkin, BET and Dubinin–Radushkevich isotherms were studied. The Langmuir isotherm model is expressed using Eq. (5).

$$q_e = \frac{q_m K_L C_e}{1 + K_L C_e} \quad (5)$$

where q_e is the amount of HA adsorbed per unit of weight of the adsorbent (mg/g), C_e is the concentration of residual HA at equilibrium time (mg/L), q_m is the maximum of adsorbed HA in unit weight of the adsorbent (mg/g) and K_L is the constant of Langmuir equation (L/mg).

One of the parameters of the Langmuir equation is R_L (coefficient of separation), which is calculated from Eq. (6). With this parameter, the type of adsorption process can be identified.

$$R_L = \frac{1}{\left(1 + bC_0\right)} \quad (6)$$

The condition $0 < R_L < 1$ indicates favorable adsorption; $1 < R_L$ is unfavorable adsorption; $R_L = 1$ indicates linear adsorption and $R_L = 0$ indicates irreversible adsorption [27].

The Freundlich adsorption isotherm equation is as follows:

$$q_e = K_f C_e^{1/n} \quad (7)$$

where C_e is the concentration of equilibrium (mg/L), n is the adsorption capacity at the time of equilibrium (mg/g), and K_f is constants of the Freundlich equation (mg/g) [28].

The Temkin isotherm is calculated by the equation as follows:

$$q_e = \frac{RT}{b_T} \ln\left(A_T C_e\right) \quad (8)$$

where b_T is the constant of the Temkin isotherm (J/mol), A_T is the constant of the Temkin isotherm (L/g), R is the global gas constant and T is the absolute temperature (K). Also, the value of B is calculated with Eq. (9).

$$B = \frac{RT}{b_T} \quad (9)$$

The BET isotherm equation is as follows:

$$q_e = \frac{q_{\max} K_b C_e}{\left(C_s - C_e\right)\left(1 + \left(K_b - 1\right)\left(\frac{C_e}{C_s}\right)\right)} \quad (10)$$

where $q_{\max}$ is the amount of adsorbed material present in the solution to form a saturation layer on the adsorbent (mg/g), K_b is reciprocal constant energy descriptor between adsorbent and adsorbate, and C_s is adsorption concentration of the adsorbing material in solution (mg/L).

The Dubinin–Radushkevich isotherm equation is as follows:

$$\varepsilon = RT \ln\left(1 + \left(\frac{1}{C_e}\right)\right) \quad (11)$$

where R is the global gas constant (8.314 J/mol.K) and T is the temperature (K) [29].

2.5. Study of adsorption kinetics

Adsorption kinetics is used to determine the control mechanism of surface adsorption processes. In order to investigate the kinetics of HA adsorption on magnetic cobalt ferrite nanoparticles, the data were matched with pseudo-first-order and pseudo-second-order models. The pseudo-first and pseudo-second-order kinetic models are as follows:

$$\frac{dq_t}{dt} = K_1\left(q_e - q_t\right) \quad (12)$$

$$\frac{dq_t}{dt} = K_2\left(q_e - q_t\right)^2 \quad (13)$$

where K_1 (1/min) is the pseudo-first-order equation and K_2 (g/mg min) is the constant of pseudo-second-order equation [30].

3. Results and discussion

3.1. Adsorbent characteristics

3.1.1. SEM analysis

The morphology of magnetic cobalt ferrite nanoparticles was investigated using SEM analysis (Fig. 2). By examining these images, it can be said that the average diameter of these nanoparticles is 50–83 nm.

3.1.2. TEM analysis

Fig. 3 shows TEM images of magnetic cobalt ferrite nanoparticles. As shown in the figure, the nanoparticle size is less than 100 nm.

3.1.3. FTIR analysis

The FTIR spectrum of magnetic cobalt ferrite nanoparticles was carried out in the range of 400–4,000 cm^{-1}. Fig. 4 shows the FTIR spectrum of cobalt ferrite magnetic nanoparticles. Specific peak points in this spectrum are as follows: 3,406 cm^{-1} (OH) and 600 and 410 cm^{-1} (presence of ferrite nanoparticles) [31].

3.1.4. XRD analysis

The XRD analysis of the magnetic cobalt ferrite nanoparticles is shown in Fig. 5. The relative positions and relative severity of all peaks are indicative of the formation of cobalt ferrite nanoparticles with a crystalline structure and in the manner of cubic spinel, which is very close to the values of the literature with the card number (JCPDS No. 01-1121) [24]. In addition, the average particle size of the nanoparticles by the Scherrer formula was calculated. The calculated size of the nanoparticles was 11 nm.

3.1.5. VSM analysis

One of the important curves reflecting the magnetic properties of the material is the hysteresis loop. Fig. 6 shows the ferromagnetic hysteresis loop of magnetic cobalt ferrite nanoparticles. As shown in this figure, the saturation magnetization (Ms) for cobalt ferrite nanoparticles is 42 emu/g.

3.2. Determination of pH_{zpc}

To determine pH_{zpc}, distilled water solutions with pH between 2 and 12 were prepared. Then, 25 mg of magnetic cobalt ferrite nanoparticles were added to 50 mL of solution. After 24 h, the pH of the solution was read. As shown in

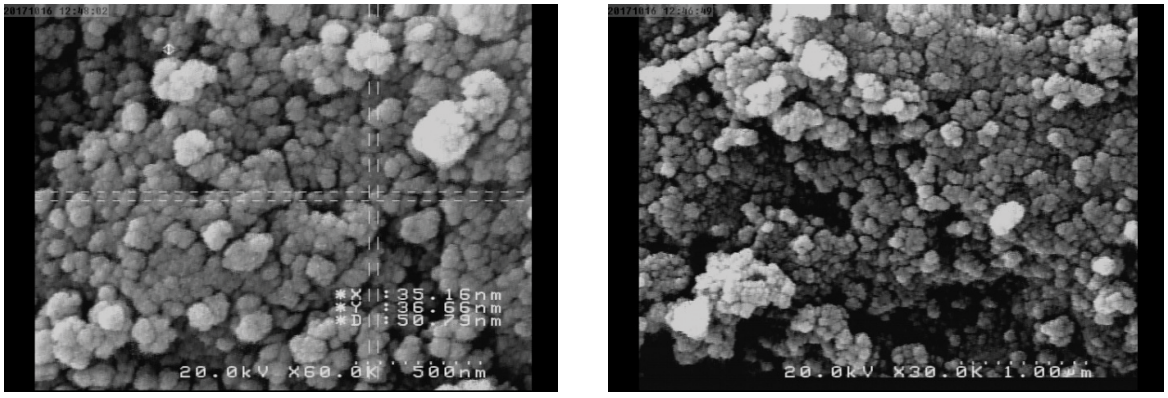

Fig. 2. SEM images of magnetic cobalt ferrite nanoparticles.

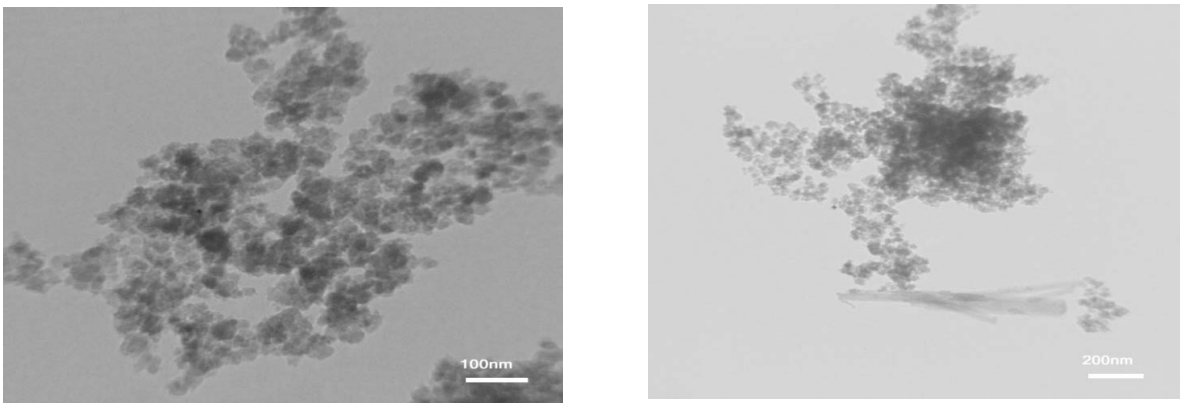

Fig. 3. TEM images of magnetic cobalt ferrite nanoparticles.

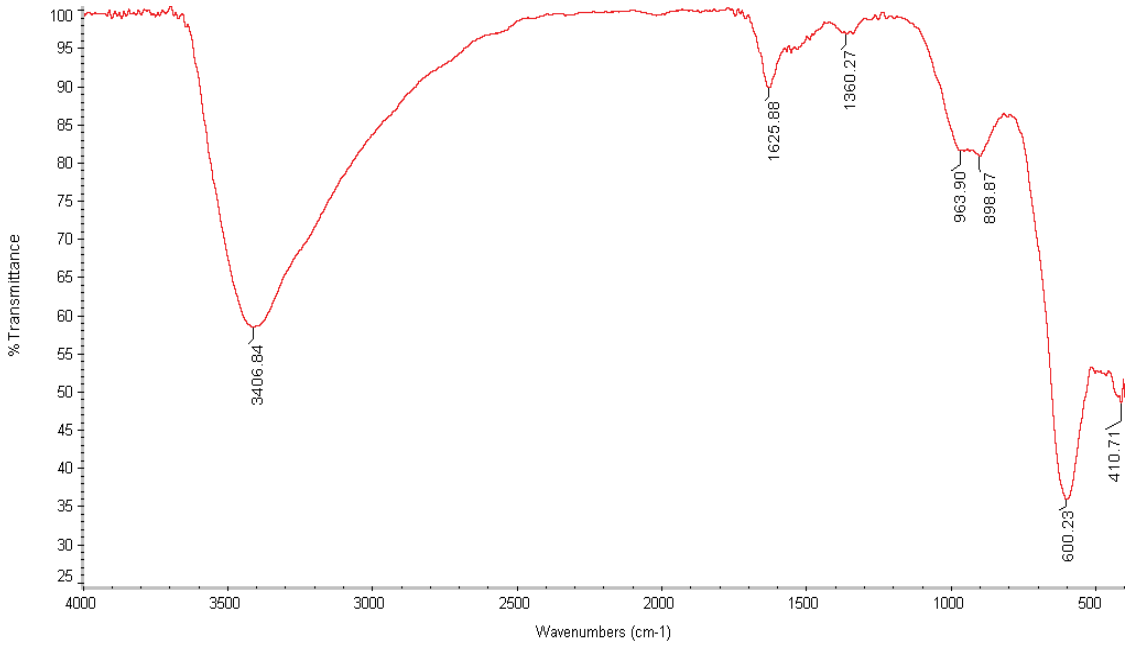

Fig. 4. FTIR spectrum of magnetic cobalt ferrite nanoparticles.

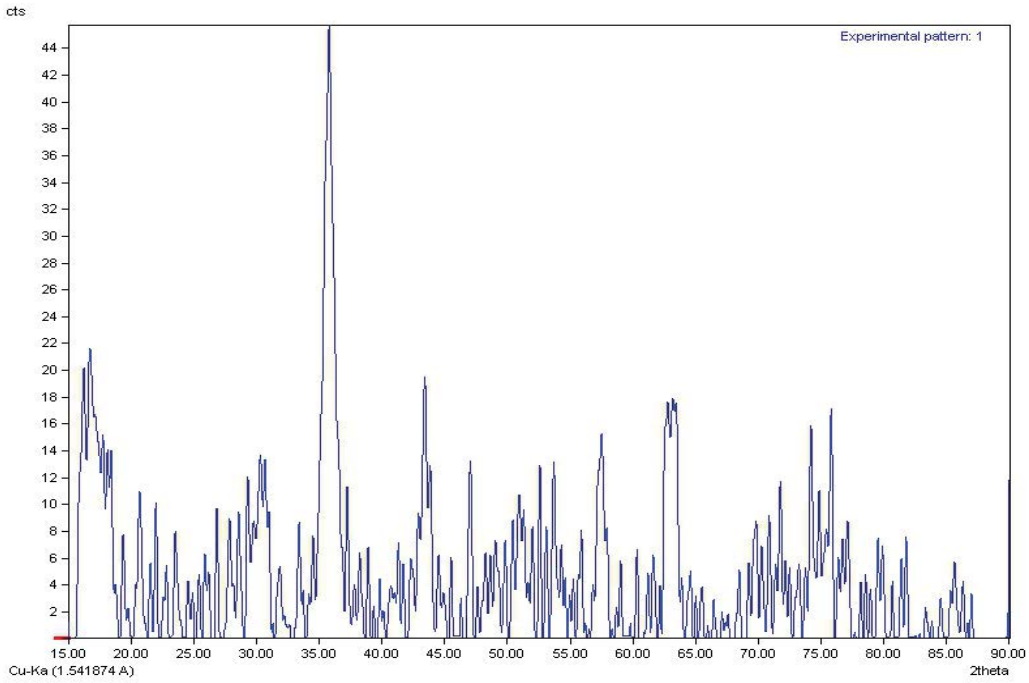

Fig. 5. XRD spectrum of magnetic cobalt ferrite nanoparticles.

Fig. 7, pH_{zpc} for cobalt ferrite magnetic nanoparticles is approximately 7.3.

3.3. *Effect of pH*

To investigate the effect of pH, HA solution with an initial concentration of 10 mg/L was prepared at different pHs of 3, 5, 7, 9, and 11. Then, 0.2 g/L of magnetic cobalt ferrite nanoparticles was added to each solution and after 60 min, the concentration of HA was determined by spectrophotometric method. As shown in Fig. 8, the amount of HA removal was higher in acidic pH. Therefore, pH = 3 was chosen as the optimal pH for the adsorption of HA. Adsorption capacity of magnetic cobalt ferrite nanoparticles at this pH was 32.9 mg/g.

One of the most important factors affecting the adsorption process is the pH of the solution and pH_{zpc}. As the results show (Fig. 8), increasing the pH of the solution from 3 to 11

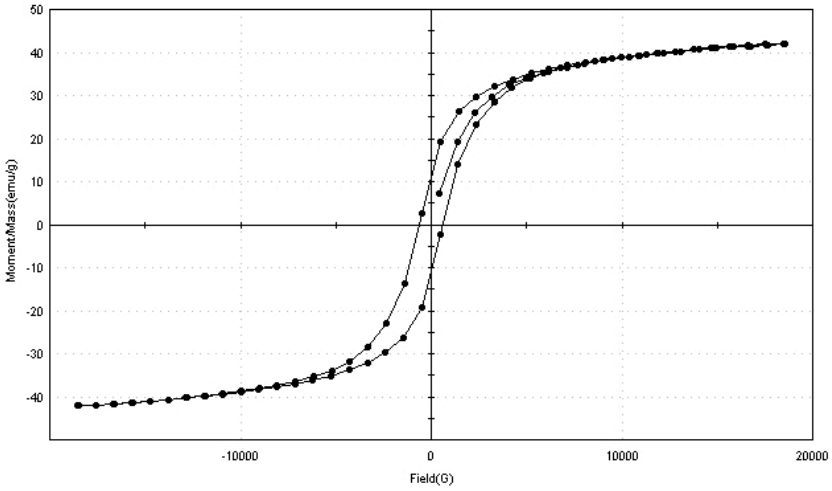

Fig. 6. VSM of magnetic cobalt ferrite nanoparticles.

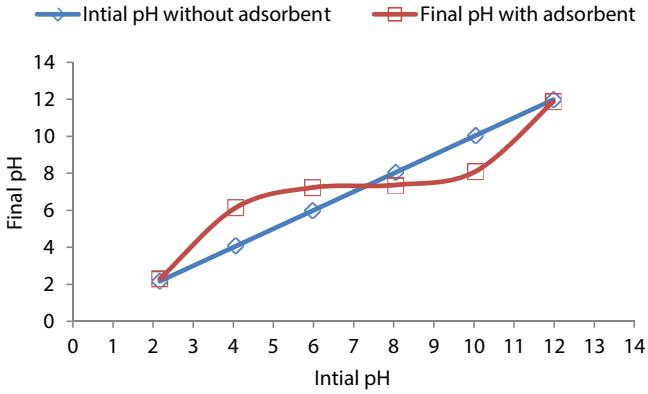

Fig. 7. pH_{zpc} of magnetic cobalt ferrite nanoparticles.

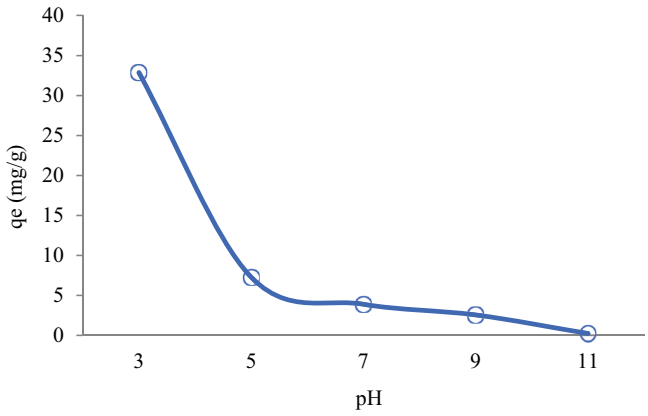

Fig. 8. Effect of pH on the removal of humic acid by magnetic cobalt ferrite nanoparticles.

decreases the rate of adsorption of HA. The reason for this is related to the structure of the anionic HA and pH_{zpc} of magnetic cobalt ferrite nanoparticles. Based on the findings of this study, pH_{zpc} for cobalt ferrite magnetic nanoparticles is about 7.3. Other studies show that at higher pHs and lower than pH_{zpc}, the adsorbents level load are often negative and positive, respectively. At pH higher than 7.3, the negative adsorption level can be attributed to the accumulation of hydroxyl anions in the adsorbent surface [32]. Therefore, in these pHs, due to the nature of the anionic HA, an electrostatic repulsive force between the adsorbent and the pollutant occurs and the rate of adsorption of HA is reduced. However, in low pHs, due to the presence of the adsorbent level and the nature of anionic HA, the rate of adsorption of HA increases. Similar results have been reported in this regard by Dong et al. [33]. These researchers reported that by increasing the pH from 4 to 10, the adsorption of HA by magnetic chitosan nanoparticle decreased [33].

3.4. Effect of adsorbent dosage

Based on the results of this study, the adsorption capacity of the magnetic cobalt ferrite nanoparticles was reduced by increasing the adsorbent dosage from 0.2 to 0.8 g/L at a HA concentration of 10 mg/L and at pH = 3 (Fig. 9). This amount decreased from 37.2 to 13.2 mg/g.

Increasing the adsorbent dose leads to more surface availability for adsorption, resulting in increased contact between the pollutant and the adsorbent [34]. On the other hand, the amount of adsorption of HA per gram of adsorbent is reduced. The reason for this is the complete lack of saturation of the adsorbent at higher dosages. This means that by increasing the adsorbent dosage, not all active sites present on the adsorbent surface are used, which leads to a decrease in the capacity for the adsorption of HAs by magnesium nanoparticles of cobalt ferrite [35]. Naghizadeh et al. [5] reported similar results for the removal of HA from walnut shell modified with TiO_2 and ZnO.

3.5. Effect of initial concentration and contact time

The results of the effect of initial concentration of HA on concentrations of 5, 10, 20, 30, and 40 mg/L of HA with pH = 3, adsorbent dosage of 0.2 g/L and in various contact times (5–90 min) is shown in Fig. 10. As shown in this figure, with the increasing in the initial concentration of HA, the adsorption capacity was increased. Also, increasing contact time has led to increased adsorption capacity. Most of the

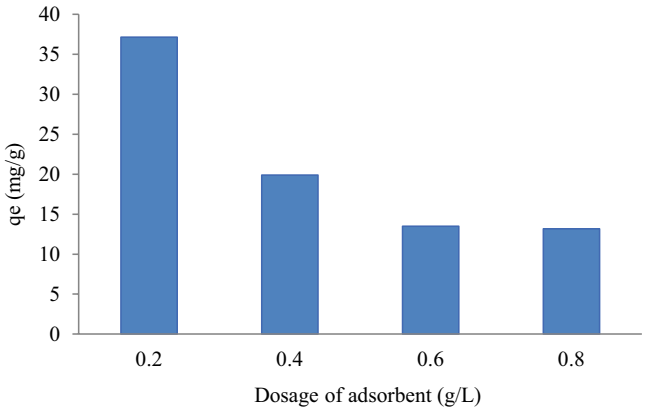

Fig. 9. Effect of adsorbent dosage on the removal of humic acid by magnetic cobalt ferrite nanoparticles.

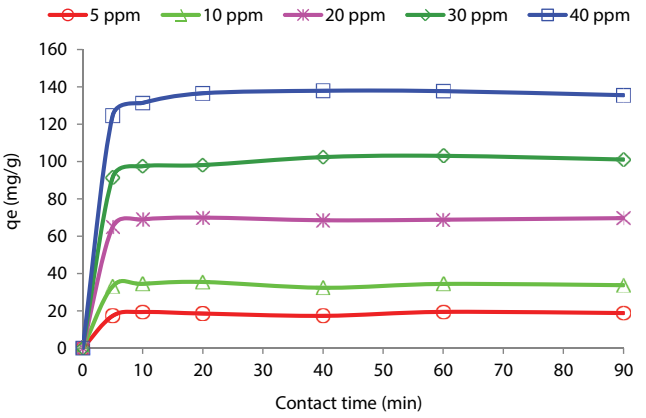

Fig. 10. Effect of initial concentration and contact time on the removal of humic acid by magnetic cobalt ferrite nanoparticles.

removal of HA by magnetic cobalt ferrite nanoparticles occurred in the early moments. According to Fig. 10, the adsorption of HA has reached a balance of about 20 min. According to the results of this stage, it is evident that at the contact time of 20 min, with an initial concentration of 5–40 mg/L, the adsorption capacity of HA was increased from 18.6 to 136.6 mg/g.

The results of this stage showed that adsorption process in this study included two stages. In the first stage, the rapid adsorption of the pollutant has occurred. But in the second stage, the rate of adsorption has been less pronounced and almost balanced afterwards. At the initial stage (during the first 20 min of adsorption), adsorption sites were more rapidly adsorbed due to the availability of adsorption sites for adsorption of HA. But in the second phase, due to the rapid rate of adsorption (quick exhaustion of adsorption sites), the adsorption rate has reached a balance. In addition, as time goes on, because of the increased repulsive force between adsorbed pollutant molecules in the surface of adsorbent, adsorption of pollutants occurs at lower vacancy levels at adsorbent surface at a lower rate. This leads to a prolonged time of adsorption or reduction in the amount of adsorption per unit time [36,37].

Also, by increasing the concentration of HA, the adsorption capacity has increased. To explain this, it can be said that by increasing the concentration of HA, massive driving force has increased, which has led to the transfer of more molecules of HA to the surface of magnetic cobalt ferrite nanoparticles [33]. In this field, a study conducted by Ngah et al. [36] confirmed the present study. In this study, it was observed that, up to 10 min, the adsorption capacity increased rapidly and then reached a balance. Also, by increasing the concentration of HA from 20 to 40 mg/L, the adsorption capacity increased [36].

3.6. Effect of temperature and thermodynamic of process

The study of the effect of temperature and thermodynamics on the process of adsorption of HA by magnetic nanoparticles of cobalt ferrite at four temperatures (283, 293, 303, and 313 K) was investigated. The results of this stage are presented in Fig. 11 and Table 1. According to Fig. 11, the temperature increase causes increase in the adsorption of HA in magnetic cobalt ferrite nanoparticles. The adsorption capacity of the magnetic cobalt ferrite nanoparticles at 283, and 313 K is 133.5, and 146.8 mg/g, respectively. To explain the reason for these results, it can be said that with increasing temperature, the mobility of HA molecules and the rate of emission of HA molecules in the surface of the adsorbent will increase, which will increase the adsorption capacity at higher temperatures. In the study conducted by Zulfikar et al. [20] on removal of HA with Fe_3O_4–chitosan hybrid nanoparticles, similar results have been obtained. Also, as shown in Table 1, the values of the parameters ΔH and ΔS are positive

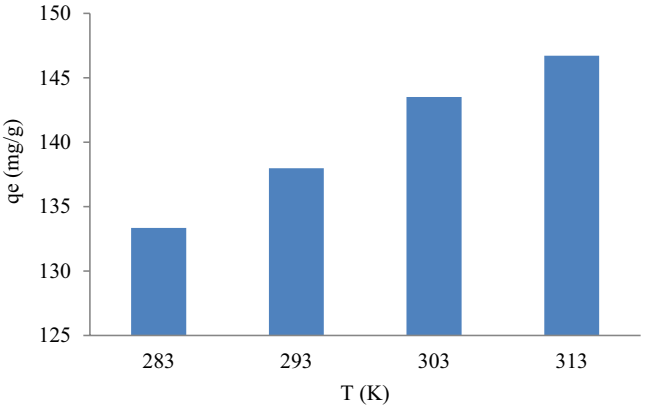

Fig. 11. Effect of temperature on the removal of humic acid by magnetic cobalt ferrite nanoparticles.

Table 1
Thermodynamic parameters of adsorption of humic acid by magnetic cobalt ferrite nanoparticles

T (K)	q_e (mg/g)	Thermodynamics parameters		
		ΔG (kJ/mol)	ΔH (kJ/mol)	ΔS (J/mol K)
283	133.35	–6.16	10.94	60.34
293	137.97	–6.70		
303	143.5	–7.37		
313	146.7	–7.90		

Table 2
Isotherm constants calculations for adsorption of humic acid onto magnetic cobalt ferrite nanoparticles

Isotherms	Constants	Values
Langmuir	q_{max} (mg/g)	491.49
	K_L (L/mg)	0.06
	R_L	0.25
	R^2	0.99
Freundlich	k_f (mg/g)	27.38
	$1/n$	0.83
	n	1.21
	R^2	0.99
BET	$1/A.X_m$	0.02
	$(A–1)/(A.X_m)$	0.08
	A	1.00
	X_m	12.59
	R^2	0.41
Temkin	A_T (L/mg)	1.82
	b_T	51.56
	B	48.06
	R^2	0.96
Dubinin–Radushkevich	β (mol²/kJ²)	0.00
	E (kJ/mol)	1.14
	q_m (mg/g)	105.41
	R^2	0.93

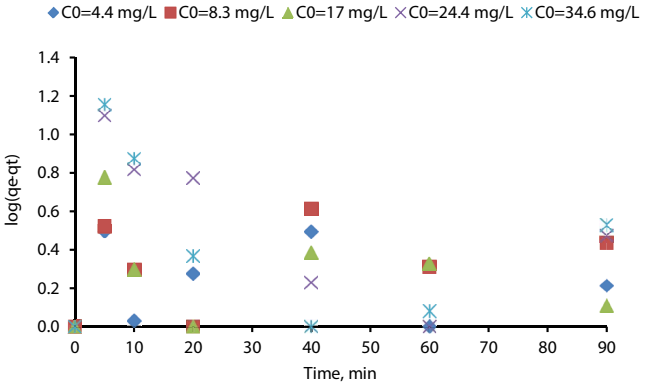

Fig. 12. Pseudo-first-order kinetic model for adsorption of the humic acid by magnetic cobalt ferrite nanoparticles.

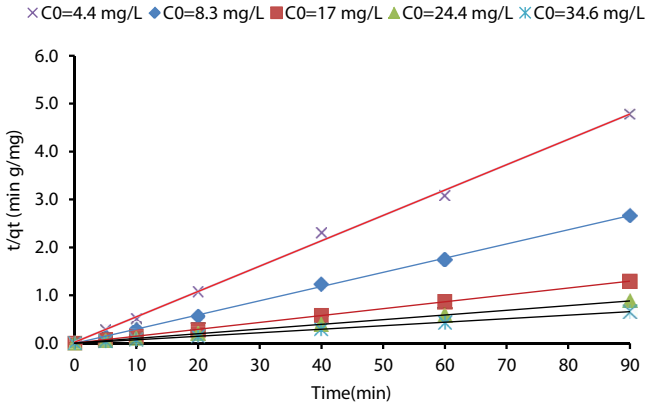

Fig. 13. Pseudo-second-order kinetic model for adsorption of the humic acid by magnetic cobalt ferrite nanoparticles.

and the values of ΔG are negative. The positive values of ΔH and ΔS indicate that the adsorption of HA with magnetic cobalt ferrite nanoparticles process is an endothermic process and therefore this process is entropy driven. Also, the negative values of ΔG indicate that the adsorption of HA on cobalt ferrite is spontaneous. In this regard, the results of Doulia et al. [38] are similar to this study.

3.7. Adsorption isotherm

Adsorption isotherm is one of the most important parameters in the design of adsorption systems to understand the adsorption mechanism [27]. In this study, the analysis of adsorption data and their correlation coefficients showed that adsorption of HA on magnetic cobalt ferrite nanoparticles follows both Langmuir and Freundlich models (R^2 = 0.99). Table 2 shows the information on adsorption isotherms. The Langmuir isotherm assumes that adsorption process occurs at the homogeneous surface, and no interaction occurs between the adsorbed molecules. The empirical Freundlich isotherm model is applicable to adsorption on heterogeneous surfaces as well as multilayer adsorption [33]. According to the results of Langmuir isotherm, R_L = 0.25. Since this value is between 0 and 1, the adsorption process is desirable. Also, in the Freundlich model, the value of $1/n$ represents the adsorption intensity. Since this number is between 1 and 10, it shows the suitability of the adsorption process [35].

Table 3
Kinetic constants calculations for adsorption of humic acid onto magnetic cobalt ferrite nanoparticles

C_0 (mg/L)	Pseudo-first-order			Pseudo-second-order			$q_{e,}$exp (mg/g)
	K_1 (min⁻¹)	$q_{e,}$cal (mg/g)	R^2	K_2 (g/mg min)	$q_{e,}$cal (mg/g)	R^2	
4.40	0.00	1.67	0.00	0.12	18.92	1.00	20.45
8.30	0.01	1.68	0.14	0.52	33.77	1.00	36.47
17.00	0.00	2.07	0.03	0.08	69.51	1.00	70.96
24.40	0.01	4.19	0.11	0.03	102.08	1.00	104.04
34.60	0.01	3.46	0.27	0.08	136.52	1.00	138.89

3.8. Adsorption kinetics

In this study, pseudo-first and pseudo-second-order kinetics were investigated. According to Figs. 12 and 13, and Table 3, pseudo-second-order kinetics has the highest correlation with the results of this study. In the second-order kinetic model, it is assumed that the adsorption process is controllable by chemical adsorption, which involves electron transfer or electron transfer between adsorbent and absorbate [16]. In this regard, the results of Li et al. [16] on the removal of HA by magnetic multi-walled carbon nanotubes decorated with calcium showed that the removal of HA follows a pseudo-second-order kinetics.

4. Conclusion

The analysis of SEM and TEM showed that the magnetic cobalt ferrite nanoparticles were below 100 nm. Also, the characteristics of magnetic cobalt ferrite nanoparticles were confirmed by FTIR and XRD analyses. Determination of the magnetic property confirmed the formation of strong magnetic nanoparticles with magnetic saturation (Ms) of 42 em/g. The results of adsorption experiments showed that the adsorption of humic acid onto magnetic cobalt ferrite nanoparticles in optimum conditions had a maximum adsorption capacity of 146.8 mg/g (optimal conditions: pH:3, adsorption dosage: 0.2 g/L, concentration of HA: 40 mg/L, contact time: 20 min, temperature: 283 K). The experimental results showed that the adsorption of HA onto magnesium magnetic cobalt ferrite nanoparticles increased at higher temperatures. Also, the results of the thermodynamics of the process showed that the values of ΔS and ΔH are positive and the value of ΔG is negative. The analysis of isotherm and adsorption kinetics models showed that the adsorption process fitted both the Langmuir and Freundlich models, as well as the pseudo-second-order kinetics.

Acknowledgment

This study was carried out in the form of a research project approved by Birjand University of Medical Sciences. The authors are grateful to the never-ending support of this university for this research.

References

[1] H. Joolaei, M. Vossoughi, A. Rashidi Mehr Abadi, A. Heravi, Removal of humic acid from aqueous solution using photocatalytic reaction on perlite granules covered by Nano TiO_2 particles, J. Mol. Liq., 242 (2017) 357–363.
[2] A.I. Zouboulis, W. Jun, I.A. Katsoyiannis, Removal of humic acids by flotation, Colloids Surf., A, 231 (2003) 181–193.
[3] M. Malakootian, K. Yaghmaeian, F. Mansoori, Effect of cations Ca^{2+} and Mg^{2+} on the removal efficiency of humic acid by UV/TiO_2, J. Shahrekord Univ. Med. Sci., 16 (2014) 9–20.
[4] Z. Yigit, H. Inan, A study of the photocatalytic oxidation of humic acid on anatase and mixed-phase anatase–rutile TiO_2 nanoparticles, Water Air Soil Pollut., 9 (2009) 237–243.
[5] A. Naghizadeh, H. Shahabi, F. Ghasemi, A. Zarei, Synthesis of walnut shell modified with titanium dioxide and zinc oxide nanoparticles for efficient removal of humic acid from aqueous solutions, J. Water Health, 14 (2016) 989–997.
[6] E. Bazrafshan, A. Joneidi Jaafari, F. Kord Mostafapour, H. Biglari, Humic acid removal from aqueous environments by electrocoagulation process duad with adding hydrogen peroxide, Iranian J. Health Environ., 5 (2012) 211–224.
[7] J. Wang, X. Han, H. Ma, Y. Ji, L. Bi, Adsorptive removal of humic acid from aqueous solution on polyaniline/attapulgite composite, Chem. Eng. J., 173 (2011) 171–177.
[8] C. Legay, M.J. Rodriguez, J.B. Sérodes, P. Levallois, Estimation of chlorination by-products presence in drinking water in epidemiological studies on adverse reproductive outcomes: a review, Sci. Total Environ., 408 (2010) 456–472.
[9] A.A. Aghapour, S. Nemati, A. Mohammadi, H. Jahani, S. Karimzadeh, Removal of Humic Acid from water resources using AL and Fe Salts during conventional coagulation, Urmia Med. J., 27 (2016) 240–247.
[10] J.-J. Qin, M.H. Oo, K.A. Kekre, F. Knops, P. Miller, Impact of coagulation pH on enhanced removal of natural organic matter in treatment of reservoir water, Sep. Purif. Technol., 49 (2006) 295–298.
[11] G. Asgari, G. Ghanizadeh, Adsorption of humic acid from aqueous solutions onto modified pumice with hexadecyl trimethyl ammonium bromide, J. Babol Univ. Med. Sci., 14 (2011) 14–22.
[12] S. Babel, P.A. Sekartaji, H. Sudrajat, TiO_2 as an effective nanocatalyst for photocatalytic degradation of humic acid in water environment, J. Water Supply Res. Technol.-Aqua, 66 (2017) 25–35.
[13] S. Wang, T. Terdkiatburana, M. Tadé, Adsorption of Cu (II), Pb (II) and humic acid on natural zeolite tuff in single and binary systems, Sep. Purif. Technol., 62 (2008) 64–70.
[14] C. Li, Y. Dong, D. Wu, L. Peng, H. Kong, Surfactant modified zeolite as adsorbent for removal of humic acid from water, Appl. Clay Sci., 52 (2011) 353–357.
[15] W. Yan, R. Bai, Adsorption of lead and humic acid on chitosan hydrogel beads, Water Res., 39 (2005) 688–698.
[16] S. Li, M. He, Z. Li, D. Li, Z. Pan, Removal of humic acid from aqueous solution by magnetic multi-walled carbon nanotubes decorated with calcium, J. Mol. Liq., 230 (2017) 520–528.
[17] J. Wang, L. Bi, Y. Ji, H. Ma, X. Yin, Removal of humic acid from aqueous solution by magnetically separable polyaniline: adsorption behavior and mechanism, J. Colloid Interface Sci., 430 (2014) 140–146.
[18] R. Bai, X. Zhang, Polypyrrole-coated granules for humic acid removal, J. Colloid Interface Sci., 243 (2001) 52–60.
[19] H. Qin, J. Meng, J. Chen, Z. You, Z. Tan, J. Ke, Adsorption of Humic Acid from Landfill Leachate by Nitrogen-Containing Activated Carbon, in: AIP Conference Proceedings, AIP Publishing, 2017, pp. 030003.
[20] M.A. Zulfikar, S. Afrita, D. Wahyuningrum, M. Ledyastuti, Preparation of Fe_3O_4-chitosan hybrid nano-particles used for humic acid adsorption, Environ. Nanotechnol. Monit. Manage., 6 (2016) 64–75.
[21] A.R. Hajipour, Z. Khorsandi, A comparative study of the catalytic activity of Co- and $CoFe_2O_4$-NPs in C-N and C-O bond formation: synthesis of benzimidazoles and benzoxazoles from o-haloanilides, New J. Chem., 40 (2016) 10474–10481.
[22] F. Zhao, Y. Zou, X. Lv, H. Liang, Q. Jia, W. Ning, Synthesis of $CoFe_2O_4$–zeolite materials and application to the adsorption of gallium and indium, J. Chem. Eng. Data, 60 (2015) 1338–1344.
[23] A.A. Rodríguez-Rodríguez, S. Martínez-Montemayor, C.C. Leyva-Porras, F.E. Longoria-Rodríguez, E. Martínez-Guerra, M. Sánchez-Domínguez, $CoFe_2O_4$-TiO_2 hybrid nanomaterials: synthesis approaches based on the oil-in-water microemulsion reaction method, J. Nanomater., 2017 (2017) 1–15.
[24] J. Saffari, D. Ghanbari, N. Mir, K. Khandan-Barani, Sonochemical synthesis of $CoFe_2O_4$ nanoparticles and their application in magnetic polystyrene nanocomposites, J. Ind. Eng. Chem., 20 (2014) 4119–4123.
[25] M. Kamranifar, M. Khodadadi, V. Samiei, B. Dehdashti, M. Noori Sepehr, L. Rafati, N. Nasseh, Comparison the removal of reactive red 195 dye using powder and ash of barberry stem as a low cost adsorbent from aqueous solutions: isotherm and kinetic study, J. Mol. Liq., 255 (2018) 572–577.
[26] H.K. Boparai, M. Joseph, D.M. O'Carroll, Kinetics and thermodynamics of cadmium ion removal by adsorption onto nano

zerovalent iron particles, J. Hazard. Mater., 186 (2011) 458–465.
[27] H. Chen, J. Zhao, J. Wu, G. Dai, Isotherm, thermodynamic, kinetics and adsorption mechanism studies of methyl orange by surfactant modified silkworm exuviae, J. Hazard. Mater., 192 (2011) 246–254.
[28] M. Kamranifar, A. Naghizadeh, Montmorillonite nanoparticles in removal of textile dyes from aqueous solutions: study of kinetics and thermodynamics, Iranian J. Chem. Chem. Eng. (IJCCE), 36 (2017) 127–137.
[29] K.Y. Foo, B.H. Hameed, Insights into the modeling of adsorption isotherm systems, Chem. Eng. J., 156 (2010) 2–10.
[30] E. Demirbas, M. Kobya, E. Senturk, T. Ozkan, Adsorption kinetics for the removal of chromium (VI) from aqueous solutions on the activated carbons prepared from agricultural wastes, Water SA, 30 (2004) 533–539.
[31] X.-H. Li, C.-L. Xu, X.-H. Han, L. Qiao, T. Wang, F.-S. Li, Synthesis and magnetic properties of nearly monodisperse $CoFe_2O_4$ nanoparticles through a simple hydrothermal condition, Nanoscale Res. Lett., 5 (2010) 1039.
[32] M. Ghaemi, G. Absalan, L. Sheikhian, Adsorption characteristics of titan yellow and Congo red on $CoFe_2O_4$ magnetic nanoparticles, J. Iranian Chem. Soc., 11 (2014) 1759–1766.
[33] C. Dong, W. Chen, C. Liu, Preparation of novel magnetic chitosan nanoparticle and its application for removal of humic acid from aqueous solution, Appl. Surface Sci., 292 (2014) 1067–1076.
[34] S. Moussavi, M. Ehrampoush, A. Mahvi, M. Ahmadian, S. Rahimi, Adsorption of humic acid from aqueous solution on single-walled carbon nanotubes, Asian J. Chem., 25 (2013) 5319.
[35] H. Abdoallahzadeh, B. Alizadeh, R. Khosravi, M. Fazlzadeh, Efficiency of EDTA modified nanoclay in removal of humic acid from aquatic solutions, J. Mazandaran Univ. Med. Sci., 26 (2016) 111–125.
[36] W.W. Ngah, S. Fatinathan, N. Yosop, Isotherm and kinetic studies on the adsorption of humic acid onto chitosan-H_2SO_4 beads, Desalination, 272 (2011) 293–300.
[37] N.Y. Mezenner, A. Bensmaili, Kinetics and thermodynamic study of phosphate adsorption on iron hydroxide-eggshell waste, Chem. Eng. J., 147 (2009) 87–96.
[38] D. Doulia, C. Leodopoulos, K. Gimouhopoulos, F. Rigas, Adsorption of humic acid on acid-activated Greek bentonite, J. Colloid Interface Sci., 340 (2009) 131–141.